Erratum: Measurement of particle production and inclusive differential cross sections in $p\bar{p}$ collisions at $\sqrt{s} = 1.96$ TeV [Phys. Rev. D 79, 112005 (2009)]

T. Aaltonen, J. Adelman, T. Akimoto, B. Álvarez González, S. Amerio, D. Amidei, A. Anastassov, A. Annovi, J. Antos, G. Apollinari, A. Apresyan, T. Arisawa, A. Artikov, W. Ashmanskas, A. Attal, A. Aurisano, F. Azfar, W. Badgett, A. Barbaro-Galtieri, V. E. Barnes, B. A. Barnett, P. Barria, V. Bartsch, G. Bauer, P.-H. Beauchemin, F. Bedeschi, D. Beecher, S. Behari, G. Bellettini, J. Bellinger, D. Benjamin, A. Beretvas, J. Beringer, A. Bhatti, M. Binkley, D. Bisello, I. Bizjak, R. E. Blair, C. Blocker, B. Blumenfeld, A. Bocci, A. Bodek, V. Boisvert, G. Bolla, D. Bortoletto, J. Boudreau, A. Boveia, B. Brau, A. Bridgeman, L. Brigliadori, C. Bromberg, E. Brubaker, J. Budagov, H. S. Budd, S. Budd, S. Burke, K. Burkett, G. Busetto, P. Bussey, A. Buzatu, K. L. Byrum, S. Cabrera, C. Calancha, M. Campanelli, M. Campbell, F. Canelli, A. Canepa, B. Carls, D. Carlsmith, R. Carosi, S. Carrillo, S. Carron, B. Casal, M. Casarsa, A. Castro, P. Catastini, D. Cauz, V. Cavaliere, M. Cavalli-Sforza, A. Cerri, L. Cerrito, S. H. Chang, Y. C. Chen, M. Chertok, G. Chiarelli, G. Chlachidze, F. Chlebana, K. Cho, D. Chokheli, J. P. Chou, G. Choudalakis, S. H. Chuang, K. Chung, W. H. Chung, Y. S. Chung, T. Chwalek, C. I. Ciobanu, M. A. Ciocci, A. Clark, D. Clark, G. Compostella, M. E. Convery, J. Conway, M. Cordelli, G. Cortiana, C. A. Cox, D. J. Cox, F. Crescioli, C. Cuenca Almenar, J. Cuevas, R. Culbertson, J. C. Cully, D. Dagenhart, M. Datta, T. Davies, P. de Barbaro, S. De Cecco, A. Deisher, G. De Lorenzo, M. Dell'Orso, C. Deluca, L. Demortier, J. Deng, M. Deninno, P. F. Derwent, A. Di Canto, G. P. di Giovanni, C. Dionisi, B. Di Ruzza, J. R. Dittmann, M. D'Onofrio, S. Donati, P. Dong, J. Donini, T. Dorigo, S. Dube, J. Efron, A. Elagin, R. Erbacher, D. Errede, S. Errede, R. Eusebi, H. C. Fang, S. Farrington, W. T. Fedorko, R. G. Feild, M. Feindt, J. P. Fernandez, C. Ferrazza, R. Field, G. Flanagan, R. Forrest, M. J. Frank, M. Franklin, J. C. Freeman, I. Furic, M. Gallinaro, J. Galyardt, F. Garberson, J. E. Garcia, A. F. Garfinkel, P. Garosi, K. Genser, H. Gerberich, D. Gerdes, A. Gessler, S. Giagu, V. Giakoumopoulou, P. Giannetti, K. Gibson, J. L. Gimmell, C. M. Ginsburg, N. Giokaris, M. Giordani, P. Giromini, M. Giunta, G. Giurgiu, V. Glagolev, D. Glenzinski, M. Gold, N. Goldschmidt, A. Golossanov, G. Gomez, G. Gomez-Ceballos, M. Goncharov, O. González, I. Gorelov, A. T. Goshaw, K. Goulianos, A. Gresele, S. Grinstein, C. Grosso-Pilcher, R. C. Group, U. Grundler, J. Guimaraes da Costa, Z. Gunay-Unalan, C. Haber, K. Hahn, S. R. Hahn, E. Halkiadakis, B.-Y. Han, J. Y. Han, F. Happacher, K. Hara, D. Hare, M. Hare, S. Harper, R. F. Harr, R. M. Harris, M. Hartz, K. Hatakeyama, C. Hays, M. Heck, A. Heijboer, J. Heinrich, C. Henderson, M. Herndon, J. Heuser, S. Hewamanage, D. Hidas, C. S. Hill, D. Hirschbuehl, A. Hocker, S. Hou, M. Houlden, S.-C. Hsu, B. T. Huffman, R. E. Hughes, U. Husemann, M. Hussein, J. Huston, J. Incandela, G. Introzzi, M. Iori, A. Ivanov, E. James, D. Jang, B. Jayatilaka, E. J. Jeon, M. K. Jha, S. Jindariani, W. Johnson, M. Jones, K. K. Joo, S. Y. Jun, J. E. Jung, T. R. Junk, T. Kamon, D. Kar, P. E. Karchin, Y. Kato, R. Kephart, W. Ketchum, J. Keung, V. Khotilovich, B. Kilminster, D. H. Kim, H. S. Kim, H. W. Kim, J. E. Kim, M. J. Kim, S. B. Kim, S. H. Kim, Y. K. Kim, N. Kimura, L. Kirsch, S. Klimenko, B. Knuteson, B. R. Ko, K. Kondo, D. J. Kong, J. Konigsberg, A. Korytov, A. V. Kotwal, M. Kreps, J. Kroll, D. Krop, N. Krumnack, M. Kruse, V. Krutelyov, T. Kubo, T. Kuhr, N. P. Kulkarni, M. Kurata, S. Kwang, A. T. Laasanen, S. Lami, S. Lammel, M. Lancaster, R. L. Lander, K. Lannon, A. Lath, G. Latino, I. Lazzizzera, T. LeCompte, E. Lee, H. S. Lee, S. W. Lee, S. Leone, J. D. Lewis, C.-S. Lin, J. Linacre, M. Lindgren, E. Lipeles, A. Lister, D. O. Litvintsev, C. Liu, T. Liu, N. S. Lockyer, A. Loginov, M. Loreti, L. Lovas, D. Lucchesi, C. Luci, J. Lueck, P. Lujan, P. Lukens, G. Lungu, L. Lyons, J. Lys, R. Lysak, D. MacQueen, R. Madrak, K. Maeshima, K. Makhoul, T. Maki, P. Maksimovic, S. Malde, S. Malik, G. Manca, A. Manousakis-Katsikakis, F. Margaroli, C. Marino, C. P. Marino, A. Martin, V. Martin, M. Martínez, R. Martínez-Ballarín, T. Maruyama, P. Mastrandrea, T. Masubuchi, M. Mathis, M. E. Mattson, P. Mazzanti, K. S. McFarland, P. McIntyre, R. McNulty, A. Mehta, P. Mehtala, A. Menzione, P. Merkel, C. Mesropian, T. Miao, N. Miladinovic, R. Miller, C. Mills, M. Milnik, A. Mitra, G. Mitselmakher, H. Miyake, N. Moggi, C. S. Moon, R. Moore, M. J. Morello, J. Morlock, P. Movilla Fernandez, J. Mülmenstädt, A. Mukherjee, Th. Muller, R. Mumford, P. Murat, M. Mussini, J. Nachtman, Y. Nagai, A. Nagano, J. Naganoma, K. Nakamura, I. Nakano, A. Napier, V. Necula, J. Nett, C. Neu, M. S. Neubauer, S. Neubauer, J. Nielsen, L. Nodulman, M. Norman, O. Norniella, E. Nurse, L. Oakes, S. H. Oh, Y. D. Oh, I. Oksuzian, T. Okusawa, R. Orava, K. Osterberg, S. Pagan Griso, E. Palencia, V. Papadimitriou, A. Papaikonomou, A. A. Paramonov, B. Parks, S. Pashapour, J. Patrick, G. Pauletta, M. Paulini, C. Paus, T. Peiffer, D. E. Pellett, A. Penzo, T. J. Phillips, G. Piacentino, E. Pianori, L. Pinera, K. Pitts, C. Plager, L. Pondrom, O. Poukhov, N. Pounder, F. Prakoshyn, A. Pronko, J. Proudfoot, F. Ptohos, E. Pueschel, G. Punzi, J. Pursley, J. Rademacker, A. Rahaman, V. Ramakrishnan, N. Ranjan, I. Redondo, P. Renton, M. Renz, M. Rescigno, S. Richter, F. Rimondi, L. Ristori, A. Robson, T. Rodrigo, T. Rodriguez, E. Rogers, S. Rolli, R. Roser, M. Rossi, R. Rossin, P. Roy, A. Ruiz, J. Russ, V. Rusu, B. Rutherford, H. Saarikko, A. Safonov, W. K. Sakumoto, O. Saltó,

1550-7998/2010/82(11)/119903(5)

L. Santi, S. Sarkar, L. Sartori, K. Sato, A. Savoy-Navarro, P. Schlabach, A. Schmidt, E. E. Schmidt, M. A. Schmidt, M. P. Schmidt, M. Schmitt, T. Schwarz, L. Scodellaro, A. Scribano, F. Scuri, A. Sedov, S. Seidel, Y. Seiya, A. Semenov, L. Sexton-Kennedy, F. Sforza, A. Sfyrla, S. Z. Shalhout, T. Shears, P. F. Shepard, M. Shimojima, S. Shiraishi, M. Shochet, Y. Shon, I. Shreyber, P. Sinervo, A. Sisakyan, A. J. Slaughter, J. Slaunwhite, K. Sliwa, J. R. Smith, F. D. Snider, R. Snihur, A. Soha, S. Somalwar, V. Sorin, T. Spreitzer, P. Squillacioti, M. Stanitzki, R. St. Denis, B. Stelzer, O. Stelzer-Chilton, D. Stentz, J. Strologas, G. L. Strycker, J. S. Suh, A. Sukhanov, I. Suslov, T. Suzuki, A. Taffard, R. Takashima, Y. Takeuchi, R. Tanaka, M. Tecchio, P. K. Teng, K. Terashi, J. Thom, A. S. Thompson, G. A. Thompson, E. Thomson, P. Tipton, P. Ttito-Guzmán, S. Tkaczyk, D. Toback, S. Tokar, K. Tollefson, T. Tomura, D. Tonelli, S. Torre, D. Torretta, P. Totaro, S. Tourneur, M. Trovato, S.-Y. Tsai, Y. Tu, N. Turini, F. Ukegawa, S. Vallecorsa, N. van Remortel, A. Varganov, E. Vataga, F. Vázquez, G. Velev, C. Vellidis, M. Vidal, R. Vidal, I. Vila, R. Vilar, T. Vine, M. Vogel, I. Volobouev, G. Volpi, P. Wagner, R. G. Wagner, R. L. Wagner, W. Wagner, J. Wagner-Kuhr, T. Wakisaka, R. Wallny, S. M. Wang, A. Warburton, D. Waters, M. Weinberger, J. Weinelt, W. C. Wester III, B. Whitehouse, D. Whiteson, A. B. Wicklund, E. Wicklund, S. Wilbur, G. Williams, H. H. Williams, P. Wilson, B. L. Winer, P. Wittich, S. Wolbers, C. Wolfe, T. Wright, X. Wu, F. Würthwein, S. Xie, A. Yagil, K. Yamamoto, J. Yamaoka, U. K. Yang, Y. C. Yang, W. M. Yao, G. P. Yeh, K. Yi, J. Yoh, K. Yorita, T. Yoshida, G. B. Yu, I. Yu, S. S. Yu, J. C. Yun, L. Zanello, A. Zanetti, X. Zhang, Y. Zheng, and S. Zucchelli

(CDF Collaboration)

(Received 18 November 2010; published 17 December 2010)

DOI: 10.1103/PhysRevD.82.119903 PACS numbers: 13.85.Hd, 99.10.Cd

The measurement of the single particle inclusive differential cross section reported in article [1] has been revised. The reported excess of high p_T prompt charged particles over PYTHIA predictions was found to be largely due to mismeasured tracks not previously taken into account.

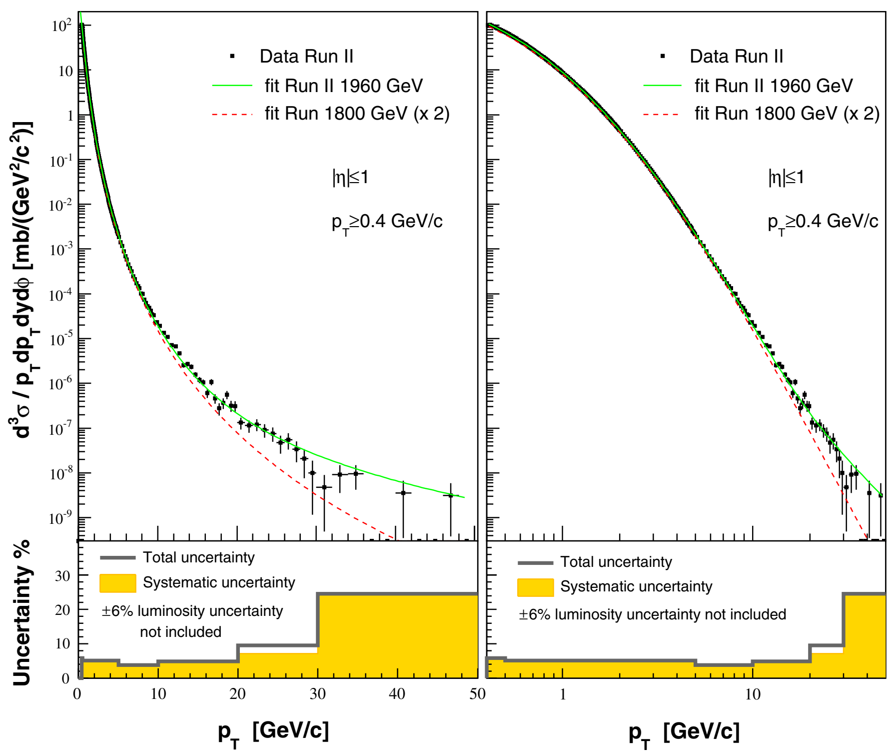

FIG. 1 (color online). The left upper plot shows the new track p_T differential cross section. The error bars describe the uncertainty on the data points. This uncertainty includes the statistical uncertainty on the data and the statistical uncertainty on the total correction. In the plots at the bottom, the systematic and the total uncertainties are shown. The total uncertainty is the quadratic sum of the uncertainty reported on the data points and the systematic uncertainty. The right-hand-side plots show the same distributions but with a logarithmic horizontal scale. Refer to article [1] for explanations about the fit.

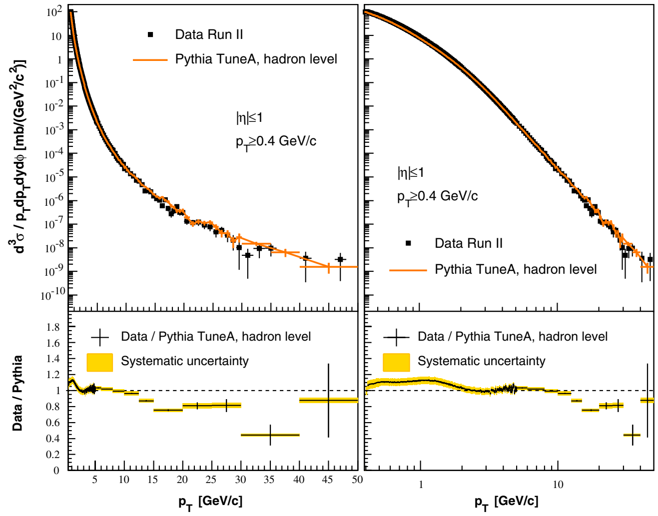

FIG. 2 (color online). The left upper plot shows a comparison of the track p_T differential cross section with the PYTHIA prediction at hadron level (Tune A with $\hat{p}_{T^0} = 1.5$ GeV/c). The data error bars describe the uncertainty on the data points. This uncertainty includes the statistical uncertainty on the data and the statistical uncertainty on the total correction. The error bars on the simulation represent its statistical uncertainty. The ratio of data over prediction is shown in the lower plots. The right-hand-side plots show the same distributions but with a logarithmic horizontal scale.

Additional studies of the effects associated with particles decaying in flight in the tracking detector volume or interacting with the detector material have led to a corrected estimate of the backgrounds due to misreconstructed tracks. These effects have been shown to affect the measurement of particle trajectories and often lead to overestimated particle momenta. The detector simulation qualitatively describes such cases, but it does not fully reproduce the magnitude of these effects. It is possible to remove misreconstructed tracks due to decays in flight and interactions with the material through a more stringent track selection procedure. In addition to the original track quality cuts in our article [1], we also require the track fit to satisfy $\chi^2/ndf < 4$. This additional requirement removes essentially all mismeasured tracks, and at the same time, it remains very efficient with respect to prompt particles. This has been confirmed in studies of muon tracks from $Z \to \mu\mu$ events. The additional efficiency correction for prompt particles based on Monte Carlo simulation is about 5%. All the other corrections remain unchanged.

The combined impact of the additional track requirements and efficiency correction is negligible for particle $p_T \lesssim 10$ GeV/c but becomes important at higher momenta and, in fact, removes all the previously observed particles with $p_T > 50$ GeV/c. The effect of additional selection requirements is found to be negligible on the measurement of the mean particle p_T as a function of the event charged particle multiplicity.

We estimate a systematic uncertainty of about 3% due to the imperfect simulation of the tracking system which leads to overly optimistic fit χ^2's. After testing three different methods to remove mismeasured trajectories, we also introduced an additional uncertainty ranging from 6% to 24% in the p_T region between 20 and 50 GeV/c.

The correct distribution (Figs. 5 and 6 of [1]) is shown in Figs. 1 and 2 of this erratum. A fit to the newly corrected data using the forms in Eq. (8) and Eq. (9) of article [1] was repeated. Tables II and III of the original article [1] are consequently modified and reported below (Tables I and II).

TABLE I. Results of the fit to the corrected data. The fit ranges only up to $p_T = 50$ GeV/c. Equation numbers refer to article [1].

	p_0	n	s	p_T range (GeV/c)	χ^2/dof
Run 0, 1800 GeV [Eq. (8)]	1.29 ± 0.02	8.26 ± 0.08	–	0.4–10	102/64
Run 0, 1800 GeV [Eq. (8)]	1.29 ± 0.02	8.26 ± 0.07	–	0.5–10	90/62
Run 0, 1800 GeV [Eq. (8)]	1.3 fixed	8.28 ± 0.02	–	0.4–10	103/65
Run II, 1960 GeV [Eq. (8)]	1.254 ± 0.004	8.15 ± 0.01	–	0.4–10	482/192
Run II, 1960 GeV [Eq. (8)]	1.244 ± 0.004	8.13 ± 0.01	–	0.5–10	309/182
Run II, 1960 GeV [Eq. (9)]	1.276 ± 0.007	8.22 ± 0.02	4.24 ± 0.07	0.4–50	555/230
Run II, 1960 GeV [Eq. (9)]	1.37 ± 0.01	8.45 ± 0.03	4.79 ± 0.02	0.5–50	227/220

TABLE II. Corrected data of inclusive single charged particle transverse momentum differential cross section.

p_T (GeV/c)	σ(mb/(GeV^2/c^2))	Stat. err.
0.40–0.41	9.914E + 01	7.2E − 01
0.41–0.42	1.011E + 02	7.3E − 01
0.42–0.43	9.721E + 01	6.2E − 01
0.43–0.44	9.307E + 01	6.0E − 01
0.44–0.45	8.886E + 01	5.8E − 01
0.45–0.46	8.483E + 01	5.6E − 01
0.46–0.47	8.097E + 01	5.4E − 01
0.47–0.48	7.783E + 01	5.2E − 01
0.48–0.49	7.460E + 01	5.0E − 01
0.49–0.50	7.126E + 01	4.8E − 01
0.50–0.51	6.805E + 01	4.6E − 01
0.51–0.52	6.508E + 01	4.5E − 01
0.52–0.53	6.231E + 01	4.3E − 01
0.53–0.54	5.949E + 01	4.1E − 01
0.54–0.55	5.665E + 01	3.9E − 01
0.55–0.56	5.418E + 01	3.8E − 01
0.56–0.57	5.175E + 01	3.6E − 01
0.57–0.58	4.947E + 01	3.5E − 01
0.58–0.59	4.726E + 01	3.3E − 01
0.59–0.60	4.504E + 01	3.2E − 01
0.60–0.61	4.319E + 01	3.1E − 01
0.61–0.62	4.113E + 01	3.0E − 01
0.62–0.63	3.940E + 01	2.8E − 01
0.63–0.64	3.760E + 01	2.7E − 01
0.64–0.65	3.605E + 01	2.6E − 01
0.65–0.66	3.448E + 01	2.5E − 01
0.66–0.67	3.300E + 01	2.4E − 01
0.67–0.68	3.159E + 01	2.3E − 01
0.68–0.69	3.033E + 01	2.2E − 01
0.69–0.70	2.894E + 01	2.1E − 01
0.70–0.71	2.777E + 01	2.0E − 01
0.71–0.72	2.661E + 01	2.0E − 01
0.72–0.73	2.557E + 01	1.9E − 01
0.73–0.74	2.447E + 01	1.8E − 01
0.74–0.75	2.346E + 01	1.7E − 01
0.75–0.76	2.255E + 01	1.7E − 01
0.76–0.77	2.165E + 01	1.6E − 01
0.77–0.78	2.075E + 01	1.6E − 01
0.78–0.79	1.989E + 01	1.5E − 01
0.79–0.80	1.915E + 01	1.4E − 01
0.80–0.81	1.847E + 01	1.4E − 01
0.81–0.82	1.769E + 01	1.3E − 01
0.82–0.83	1.696E + 01	1.3E − 01
0.83–0.84	1.633E + 01	1.2E − 01
0.84–0.85	1.571E + 01	1.2E − 01
0.85–0.86	1.506E + 01	1.1E − 01
0.86–0.87	1.450E + 01	1.1E − 01
0.87–0.88	1.396E + 01	1.1E − 01
0.88–0.89	1.347E + 01	1.0E − 01
0.89–0.90	1.290E + 01	1.0E − 01
0.90–0.91	1.244E + 01	9.6E − 02
0.91–0.92	1.199E + 01	9.3E − 02
0.92–0.93	1.151E + 01	9.0E − 02
0.93–0.94	1.112E + 01	8.7E − 02
0.94–0.95	1.068E + 01	8.2E − 02
0.95–0.96	1.029E + 01	8.1E − 02
0.96–0.97	9.979E + 00	7.8E − 02
0.97–0.98	9.587E + 00	7.5E − 02
0.98–0.99	9.275E + 00	7.3E − 02
0.99–1.00	8.907E + 00	7.0E − 02
1.00–1.02	8.462E + 00	6.3E − 02
1.02–1.04	7.885E + 00	5.9E − 02
1.04–1.06	7.338E + 00	5.6E − 02
1.06–1.08	6.835E + 00	5.2E − 02
1.08–1.10	6.380E + 00	4.9E − 02
1.10–1.12	5.958E + 00	4.6E − 02
1.12–1.14	5.576E + 00	4.3E − 02
1.14–1.16	5.220E + 00	4.0E − 02
1.16–1.18	4.862E + 00	3.8E − 02
1.18–1.20	4.557E + 00	3.6E − 02
1.20–1.22	4.266E + 00	3.3E − 02
1.22–1.24	3.990E + 00	3.2E − 02
1.24–1.26	3.740E + 00	3.0E − 02
1.26–1.28	3.527E + 00	2.8E − 02
1.28–1.30	3.301E + 00	2.6E − 02
1.30–1.32	3.092E + 00	2.5E − 02
1.32–1.34	2.911E + 00	2.3E − 02
1.34–1.36	2.727E + 00	2.2E − 02
1.36–1.38	2.568E + 00	2.1E − 02
1.38–1.40	2.412E + 00	2.0E − 02
1.40–1.42	2.275E + 00	1.9E − 02
1.42–1.44	2.133E + 00	1.8E − 02
1.44–1.46	2.014E + 00	1.7E − 02
1.46–1.48	1.894E + 00	1.6E − 02
1.48–1.50	1.794E + 00	1.5E − 02
1.50–1.52	1.689E + 00	1.4E − 02
1.52–1.54	1.599E + 00	1.4E − 02
1.54–1.56	1.500E + 00	1.3E − 02
1.56–1.58	1.414E + 00	1.3E − 02
1.58–1.60	1.341E + 00	1.2E − 02
1.60–1.62	1.264E + 00	1.1E − 02
1.62–1.64	1.202E + 00	1.1E − 02
1.64–1.66	1.131E + 00	1.0E − 02
1.66–1.68	1.073E + 00	9.6E − 03
1.68–1.70	1.017E + 00	9.1E − 03
1.70–1.72	9.578E − 01	8.7E − 03
1.72–1.74	9.041E − 01	8.2E − 03
1.74–1.76	8.613E − 01	7.9E − 03
1.76–1.78	8.187E − 01	7.5E − 03
1.78–1.80	7.737E − 01	7.1E − 03
1.80–1.82	7.322E − 01	6.8E − 03
1.82–1.84	6.924E − 01	6.4E − 03
1.84–1.86	6.594E − 01	6.2E − 03
1.86–1.88	6.249E − 01	6.0E − 03
1.88–1.90	5.923E − 01	5.7E − 03
1.90–1.92	5.648E − 01	5.4E − 03
1.92–1.94	5.337E − 01	5.2E − 03
1.94–1.96	5.110E − 01	5.0E − 03
1.96–1.98	4.867E − 01	4.8E − 03
1.98–2.00	4.584E − 01	4.6E − 03
2.00–2.05	4.231E − 01	3.8E − 03
2.05–2.10	3.720E − 01	3.3E − 03
2.10–2.15	3.295E − 01	3.0E − 03
2.15–2.20	2.930E − 01	2.6E − 03
2.20–2.25	2.607E − 01	2.4E − 03
2.25–2.30	2.320E − 01	2.2E − 03
2.30–2.35	2.069E − 01	2.0E − 03
2.35–2.40	1.840E − 01	1.8E − 03
2.40–2.45	1.656E − 01	1.6E − 03
2.45–2.50	1.479E − 01	1.5E − 03
2.50–2.55	1.319E − 01	1.4E − 03
2.55–2.60	1.180E − 01	1.2E − 03
2.60–2.65	1.067E − 01	1.1E − 03

TABLE II. (*Continued*)

p_T (GeV/c)	σ(mb/(GeV^2/c^2))	Stat. err.
2.65–2.70	9.53E − 02	1.0E − 03
2.70–2.75	8.748E − 02	9.6E − 04
2.75–2.80	7.783E − 02	8.7E − 04
2.80–2.85	7.071E − 02	7.8E − 04
2.85–2.90	6.330E − 02	7.3E − 04
2.90–2.95	5.728E − 02	6.7E − 04
2.95–3.00	5.264E − 02	6.1E − 04
3.00–3.05	4.759E − 02	5.6E − 04
3.05–3.10	4.327E − 02	5.3E − 04
3.10–3.15	3.934E − 02	5.1E − 04
3.15–3.20	3.557E − 02	4.5E − 04
3.20–3.25	3.186E − 02	4.1E − 04
3.25–3.30	2.992E − 02	4.1E − 04
3.30–3.35	2.709E − 02	3.7E − 04
3.35–3.40	2.497E − 02	3.5E − 04
3.40–3.45	2.259E − 02	3.2E − 04
3.45–3.50	2.053E − 02	2.9E − 04
3.50–3.55	1.924E − 02	2.8E − 04
3.55–3.60	1.740E − 02	2.6E − 04
3.60–3.65	1.630E − 02	2.5E − 04
3.65–3.70	1.490E − 02	2.3E − 04
3.70–3.75	1.365E − 02	2.1E − 04
3.75–3.80	1.270E − 02	2.0E − 04
3.80–3.85	1.160E − 02	1.9E − 04
3.85–3.90	1.073E − 02	1.8E − 04
3.90–3.95	9.88E − 03	1.7E − 04
3.95–4.00	9.07E − 03	1.6E − 04
4.00–4.05	8.55E − 03	1.5E − 04
4.05–4.10	7.93E − 03	1.4E − 04
4.10–4.15	7.13E − 03	1.4E − 04
4.15–4.20	6.82E − 03	1.3E − 04
4.20–4.25	6.30E − 03	1.2E − 04
4.25–4.30	5.74E − 03	1.1E − 04
4.30–4.35	5.36E − 03	1.1E − 04
4.35–4.40	4.91E − 03	1.0E − 04
4.40–4.45	4.629E − 03	9.7E − 05
4.45–4.50	4.314E − 03	9.4E − 05
4.50–4.55	3.920E − 03	9.0E − 05
4.55–4.60	3.743E − 03	8.3E − 05
4.60–4.65	3.374E − 03	8.0E − 05
4.65–4.70	3.309E − 03	7.6E − 05
4.70–4.75	3.102E − 03	7.3E − 05
4.75–4.80	2.877E − 03	7.0E − 05
4.80–4.85	2.546E − 03	6.4E − 05
4.85–4.90	2.457E − 03	6.2E − 05
4.90–4.95	2.289E − 03	5.9E − 05
4.95–5.00	2.150E − 03	5.7E − 05
5.00–5.20	1.879E − 03	3.3E − 05
5.20–5.40	1.422E − 03	2.8E − 05
5.40–5.60	1.159E − 03	2.2E − 05
5.60–5.80	8.91E − 04	1.9E − 05
5.80–6.00	6.97E − 04	1.6E − 05
6.00–6.20	5.86E − 04	1.4E − 05
6.20–6.40	4.56E − 04	1.2E − 05
6.40–6.60	3.78E − 04	1.0E − 05
6.60–6.80	3.144E − 04	9.2E − 06
6.80–7.00	2.482E − 04	8.2E − 06
7.00–7.20	2.109E − 04	7.1E − 06
7.20–7.40	1.736E − 04	6.2E − 06
7.40–7.60	1.480E − 04	5.6E − 06
7.60–7.80	1.347E − 04	5.2E − 06
7.80–8.00	1.009E − 04	4.7E − 06
8.00–8.20	9.89E − 05	4.3E − 06
8.20–8.40	7.34E − 05	3.6E − 06
8.40–8.60	6.20E − 05	3.2E − 06
8.60–8.80	5.27E − 05	2.9E − 06
8.80–9.00	4.86E − 05	2.7E − 06
9.00–9.20	4.20E − 05	2.5E − 06
9.20–9.40	3.48E − 05	2.2E − 06
9.40–9.60	3.35E − 05	2.2E − 06
9.60–9.80	2.27E − 05	1.7E − 06
9.80–10.00	2.34E − 05	1.8E − 06
10.00–10.50	1.92E − 05	1.0E − 06
10.50–11.00	1.358E − 05	8.3E − 07
11.00–11.50	1.087E − 05	7.2E − 07
11.50–12.00	7.21E − 06	5.7E − 07
12.00–12.50	6.69E − 06	5.3E − 07
12.50–13.00	4.65E − 06	4.3E − 07
13.00–13.50	2.57E − 06	3.0E − 07
13.50–14.00	2.69E − 06	3.1E − 07
14.00–14.50	2.35E − 06	2.8E − 07
14.50–15.00	1.56E − 06	2.2E − 07
15.00–15.50	1.20E − 06	1.9E − 07
15.50–16.00	1.05E − 06	1.8E − 07
16.00–16.50	6.1E − 07	1.3E − 07
16.50–17.00	1.08E − 06	1.7E − 07
17.00–17.50	4.6E − 07	1.1E − 07
17.50–18.00	2.76E − 07	8.5E − 08
18.00–18.50	3.67E − 07	9.8E − 08
18.50–19.00	5.6E − 07	1.2E − 07
19.00–19.50	3.19E − 07	8.8E − 08
19.50–20.00	3.12E − 07	8.6E − 08
20.00–21.00	1.32E − 07	3.9E − 08
21.00–22.00	1.14E − 07	3.5E − 08
22.00–23.00	1.21E − 07	3.6E − 08
23.00–24.00	9.14E − 08	3.0E − 08
24.00–25.00	7.62E − 08	2.7E − 08
25.00–26.00	4.78E − 08	2.1E − 08
26.00–27.00	5.5E − 08	2.2E − 08
27.00–28.00	3.4E − 08	1.7E − 08
28.00–29.00	2.1E − 08	1.3E − 08
29.00–30.00	1.00E − 08	8.9E − 09
30.00–32.00	4.7E − 09	4.2E − 09
32.00–34.00	9.2E − 09	5.7E − 09
34.00–36.00	9.5E − 09	5.3E − 09
36.00–38.00	0.000E + 00	0.0E + 00
38.00–40.00	0.000E + 00	0.0E + 00
40.00–42.00	3.5E − 09	3.2E − 09
42.00–44.00	0.000E + 00	0.0E + 00
44.00–46.00	0.000E + 00	0.0E + 00
46.00–48.00	3.2E − 09	2.8E − 09
48.00–50.00	0.000E + 00	0.0E + 00

[1] T. Aaltonen *et al.* (CDF Collaboration), Phys. Rev. D 79, 112005 (2009).